

*Supplementary Materials*

# Limitations Imposed Using an Iodide/Triiodide Redox Couple in Solar-Powered Electrochromic Devices

George Syrrakostas \*, Sarantis Tsamoglou and George Leftheriotis

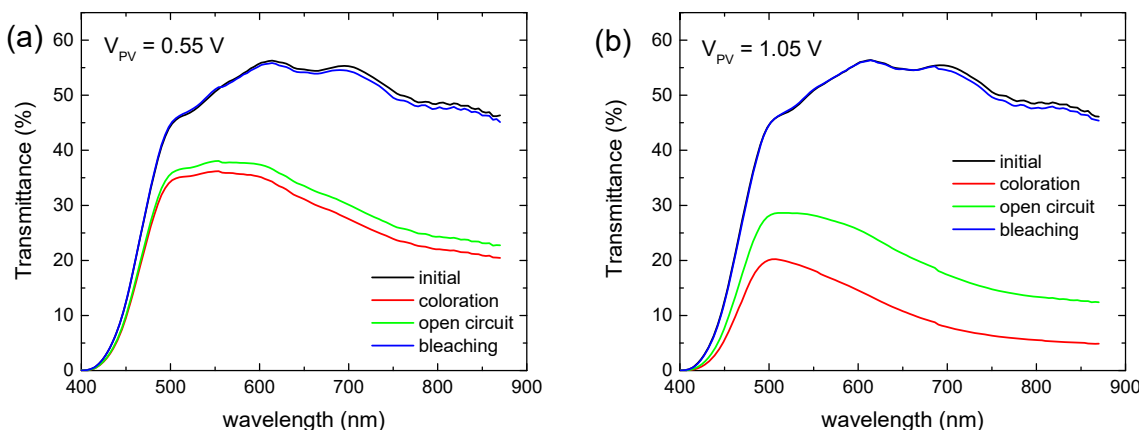
Renewable Energy Laboratory, Department of Physics, University of Patras, GR-26504 Patra, Greece;  
tsamogloys@gmail.com (S.T.) glefther@upatras.gr (G.L.)

\* Correspondence: gesirrokos@upatras.gr

**Table S1.** Comparative table with hybrid ECDs having different redox electrolytes.

Redox Couple	Optical Modulation ( $\Delta T$ )	Bias Potential	Switching Time (s)	Nr of Cycles/Operation Time	Ref.
I <sup>-</sup> / I <sub>3</sub> <sup>-</sup>	61.8% (visual)	- 2V / +0.5 V	8*		[1]
Thiolate/disulphide (T/T <sub>2</sub> )	52 % at 550 nm		28 / 15**	50 cycles	[2]
I <sup>-</sup> / I <sub>3</sub> <sup>-</sup>	45 % at 550 nm	- 2.5 V / + 1.0 V	5 / 23**		[2]
Fc <sup>+</sup> / Fc	52 %	- 1.5V / 0 V	10 / 22**	10 h	[3]
TMTU/TMFDS <sup>2+</sup>	67.8 % at 648 nm	- 1.2 V / 1.0 V	7.3 / 5.9	> 100,000 cycles	[4]
I <sup>-</sup> / I <sub>3</sub> <sup>-</sup>	44.3 % (vis)	- 1 V	-		[5]
TMTU/TMFDS <sup>2+</sup>	68 % (vis)	- 1 V	-		[5]
TMTU/TMFDS <sup>2+</sup>	55 % (vis)	- 1.5 V / 1.5 V	< 5 min		[6]
I <sup>-</sup> / I <sub>3</sub> <sup>-</sup>	42.9 % (vis)	-0.72 V / 0.6 V			[7]
TMTU/TMFDS <sup>2+</sup>	57.2 % (vis)	-0.795 V / 0.6 V	5 min		[7]
TEMPO/TEMPO <sup>+</sup>	31.4 % (vis)	-1.035 V / 0.6 V			[7]
TMTU/TMFDS <sup>2+</sup>	32 % (vis)	-2 V / 2 V			[8]
TTF	93 %	-0.9 V / no bias	12 / 28 **	200 cycles	[9]
I <sup>-</sup> / I <sub>3</sub> <sup>-</sup>	30 – 35 % at 634 nm	- 1.5 V / 1.7 V	60 / 60	11,000 cycles	[10]
TMTU/TMFDS <sup>2+</sup>	68.2 % at 603 nm	-1.5 V / 1.2 V	12.8 / 5.3**	10,000 cycles	[11]
I <sup>-</sup> / I <sub>3</sub> <sup>-</sup>	59.4 %	- 1.8 V / 1.2 V	3.1 / 1.9**		[12]
I <sup>-</sup> / I <sub>3</sub> <sup>-</sup>					Our work

\*: the time to achieve a reduction of the transmittance by a factor of 10; \*\*:  $t_c$  and  $t_b$  represents the time to modulate the 90% of the maximum  $\Delta T$ .



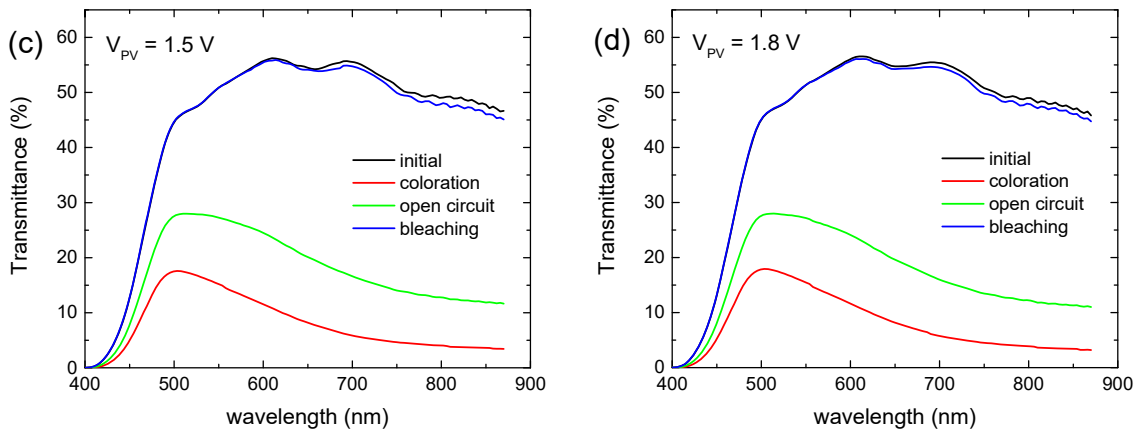


**Figure S1.** Transmittance spectra of a hybrid ECD during a coloration – bleaching cycle for the different values of the applied bias potential ( $V_{PV}$ ), which was increased using series connected mini silicon solar cells: (a) 1 mini silicon solar cell, (b) 2 mini silicon solar cells, (c) 3 mini silicon solar cells and (d) 4 mini silicon solar cells.

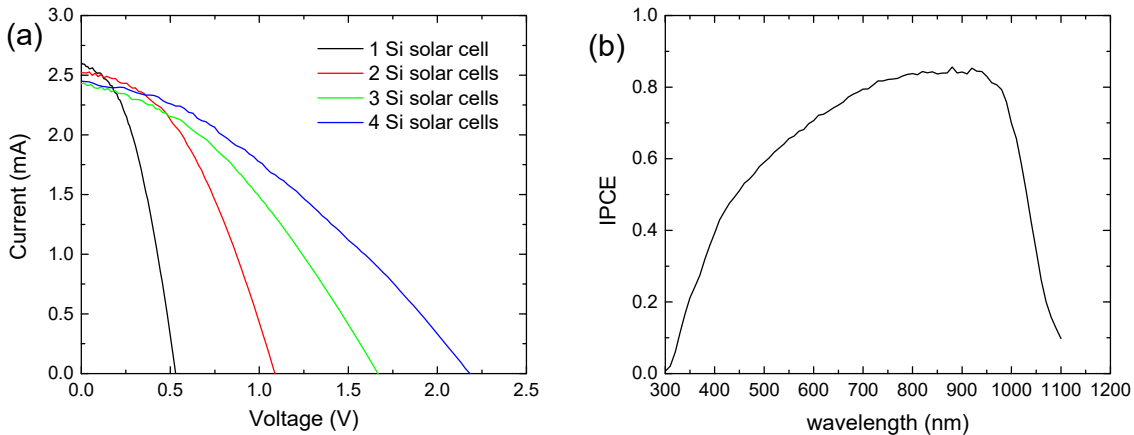


**Figure S2.** (a) Typical I-V curves of up to 4 series connected BPW34 mini-Si solar cells and (b) a typical IPCE spectrum.

**Table S2.** Characteristic photovoltaic properties of series connected BPW34 mini silicon solar cells.

	V <sub>oc</sub> (V)	I <sub>sc</sub> (mA)	FF	PCE (%)
1 Si solar cell	0.532	2.60	0.421	12.9
2 Si solar cells	1.09	2.52	0.421	13.0
3 Si solar cells	1.68	2.43	0.366	12.1
4 Si solar cells	2.19	2.45	0.345	11.1

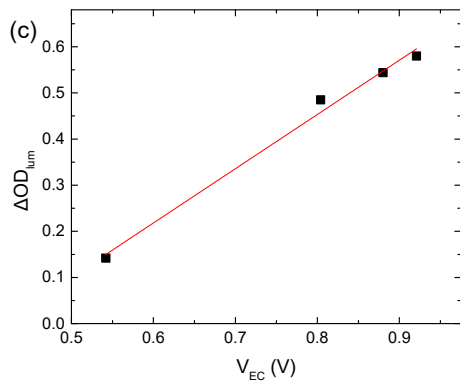
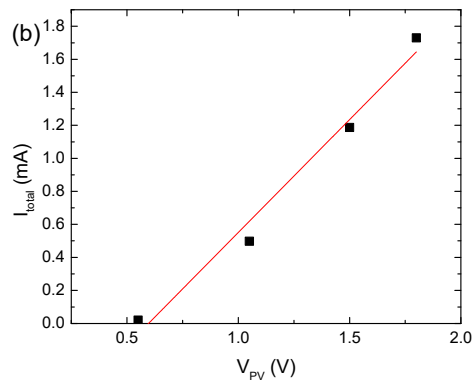
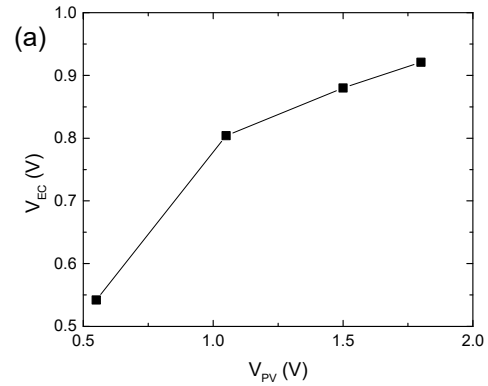


**Figure S3.** (a) Variation in the voltage at the ECD terminals ( $V_{EC}$ ) with respect to the applied bias potential ( $V_{PV}$ ), (b) linear increment in  $I_{total}$  passing through of the ECD with the applied bias potential ( $V_{PV}$ ), (c) linear increment in the luminous optical density modulation with the voltage at the ECD terminals ( $V_{EC}$ ).

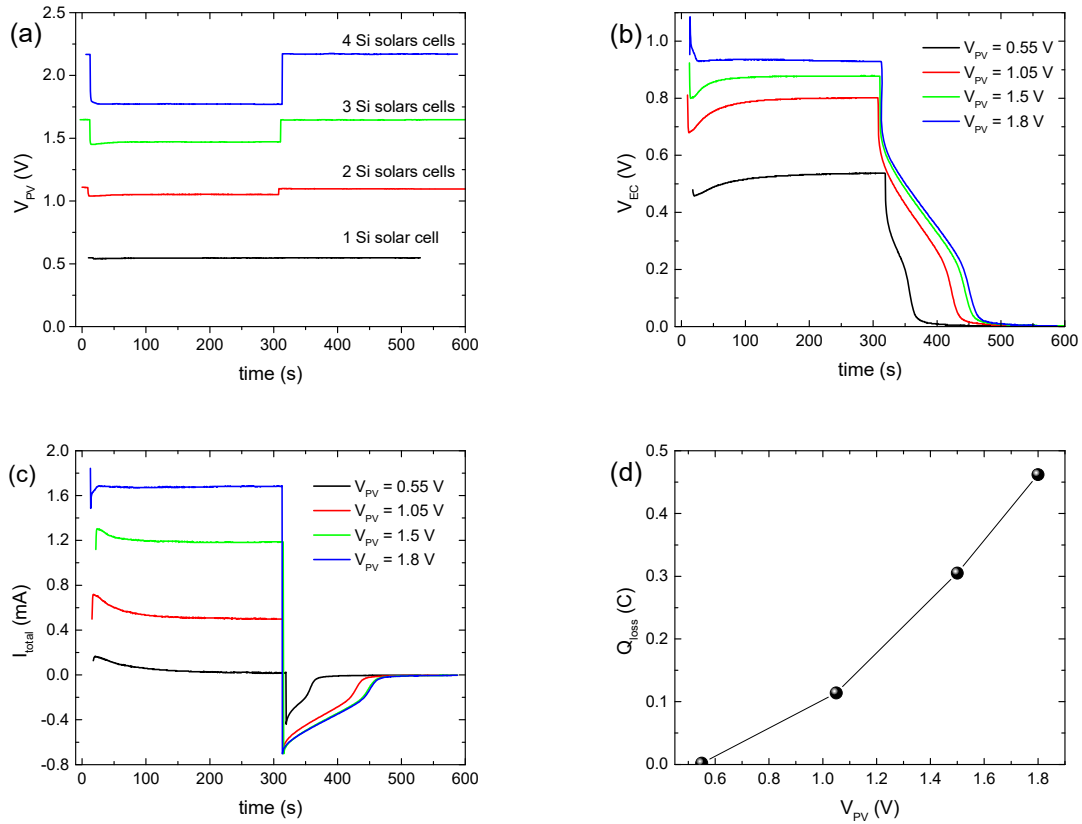


**Figure S4.** Variation in the applied bias potential  $V_{PV}$  (a), the potential at the terminals of the ECD ( $V_{EC}$ ) (b) and the total current density ( $I_{total}$ ) passing through the ECD (c) during a coloration–bleaching cycle, (d) variation in  $Q_{loss}$  with the applied bias potential ( $V_{PV}$ ).

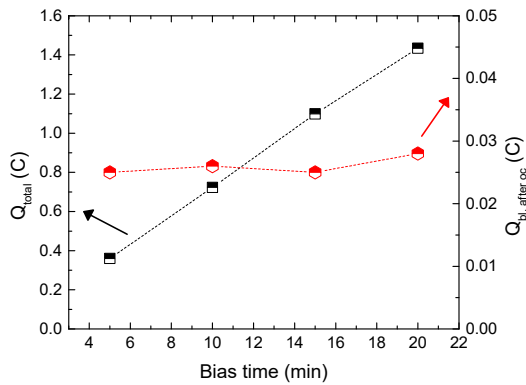


**Figure S5.** Variation in the total charge ( $Q_{total}$ ) and the charge released from the  $\text{WO}_3$  layer during bleaching ( $Q_{bl, \text{after } oc}$ ) with the bias time, after an open circuit step.

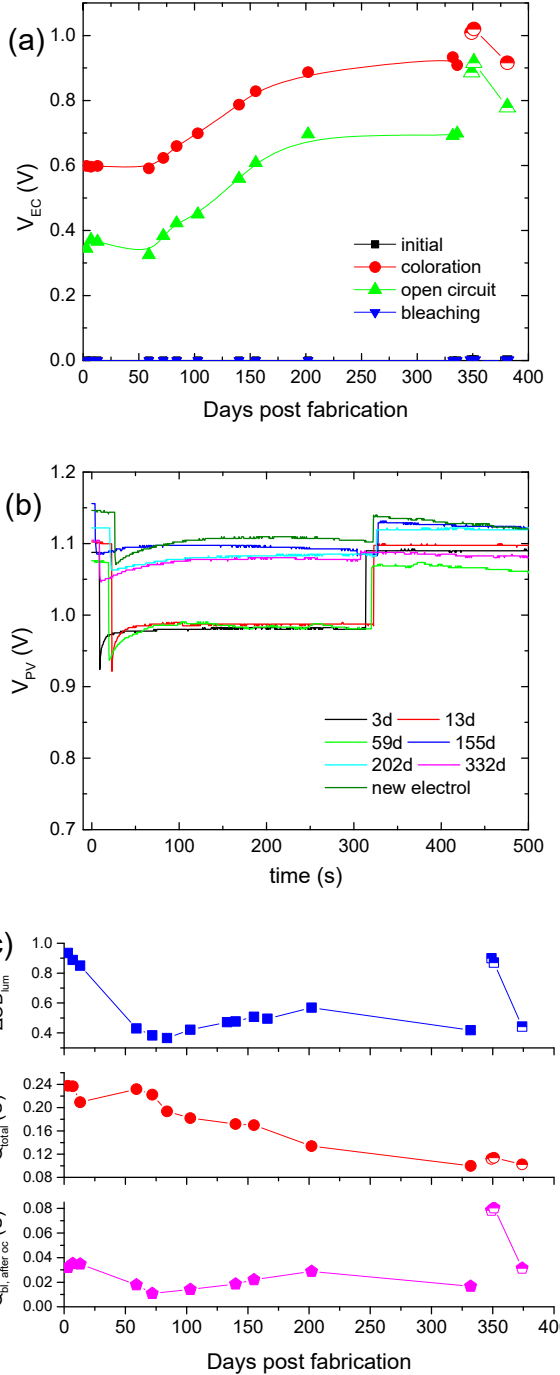


**Figure S6.** (a) Variation in the potential at the terminals of the ECD ( $V_{EC}$ ) at the end of each step during a coloration–bleaching cycle with days post-fabrication, (b) variation in the applied bias potential ( $V_{PV}$ ) for specific days post-fabrication during coloration of the ECD, (c) variation in  $\Delta OD_{lum}$ ,  $Q_{total}$  and  $Q_{bl, after\;oc}$  with days post-fabrication. (open symbols are used in the case of the fresh electrolyte).

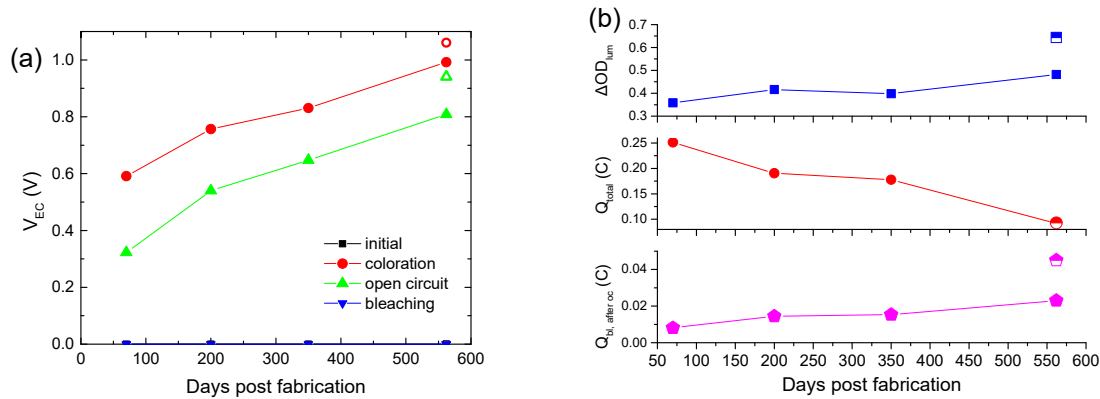


**Figure S7.** (a) Variation in the potential at the terminals of the ECD ( $V_{EC}$ ) at the end of each step during a coloration–bleaching cycle with days post-fabrication, (b) variation in  $\Delta OD_{lum}$ ,  $Q_{total}$  and  $Q_{bol}$  after  $oc$  with days post-fabrication. (open symbols are used in the case of the fresh electrolyte).

## References:

1. A.A.A. Georg, A.A.A. Georg, Electrochromic device with a redox electrolyte, Sol. Energy Mater. Sol. Cells. 93 (2009) 1329–1337. doi:10.1016/j.solmat.2009.02.009.
2. R. Giannuzzi, C.T. Prontera, V. Primiceri, A.L. Capodilupo, M. Pugliese, F. Mariano, A. Maggiore, G. Gigli, V. Maiorano, Hybrid electrochromic device with transparent electrolyte, Sol. Energy Mater. Sol. Cells. 257 (2023) 112346. doi:10.1016/j.solmat.2023.112346.
3. J. Bae, H. Kim, H.C. Moon, S.H. Kim, Low-voltage, simple WO<sub>3</sub> -based electrochromic devices by directly incorporating an anodic species into the electrolyte, J. Mater. Chem. C. 4 (2016) 10887–10892. doi:10.1039/C6TC03463B.
4. Z. Wang, K. Shen, H. Xie, B. Xue, J. Zheng, C. Xu, Robust non-complementary electrochromic device based on WO<sub>3</sub> film and CoS catalytic counter electrode with TMTU/TMFDS<sub>2+</sub> redox couple, Chem. Eng. J. 426 (2021) 131314. doi:10.1016/j.cej.2021.131314.
5. S. Bogati, A. Georg, W. Graf, Sputtered Si<sub>3</sub>N<sub>4</sub> and SiO<sub>2</sub> electron barrier layer between a redox electrolyte and the WO<sub>3</sub> film in electrochromic devices, Sol. Energy Mater. Sol. Cells. 159 (2017) 395–404. doi:10.1016/j.solmat.2016.08.023.
6. M. Hočevá, U. Opara Krašovec, Solid electrolyte containing a colorless redox couple for electrochromic device, Sol. Energy Mater. Sol. Cells. 196 (2019) 9–15. doi:10.1016/j.solmat.2019.03.027.
7. S. Bogati, A. Georg, C. Jerg, W. Graf, Tetramethylthiourea (TMTU) as an alternative redox mediator for electrochromic devices, Sol. Energy Mater. Sol. Cells. 157 (2016) 454–461. doi:10.1016/j.solmat.2016.07.023.
8. L. Niklaus, M. Schott, U. Posset, G.A. Giffin, Redox Electrolytes for Hybrid Type II Electrochromic Devices with Fe–MEPE or Ni 1 – x O as Electrode Materials, ChemElectroChem. 7 (2020) 3274–3283. doi:10.1002/celc.202000583.
9. Y.M. Kim, X. Li, K.-W. Kim, S.H. Kim, H.C. Moon, Tetrathiafulvalene: effective organic anodic materials for WO<sub>3</sub> -based electrochromic devices, RSC Adv. 9 (2019) 19450–19456. doi:10.1039/C9RA02840D.
10. M. Čolović, M. Hajzeri, M. Tramšek, B. Orel, A.K. Surca, In situ Raman and UV-visible study of hybrid electrochromic devices with bis end-capped designed trialkoxysilyl-functionalized ionic liquid based electrolytes, Sol. Energy Mater. Sol. Cells. 220 (2021) 110863. doi:10.1016/j.solmat.2020.110863.
11. Y. Ke, Z. Wang, H. Xie, M.A. Khalifa, J. Zheng, C. Xu, Long-Term Stable Complementary Electrochromic Device Based on WO<sub>3</sub> Working Electrode and NiO-Pt Counter Electrode, Membranes (Basel). 13 (2023) 601. doi:10.3390/membranes13060601.
12. S.M. Wang, Y. Wang, T. Wang, Z. Han, C. Cho, E. Kim, Charge-Balancing Redox Mediators for High Color Contrast Electrochromism on Polyoxometalates, Adv. Mater. Technol. 5 (2020) 1–9. doi:10.1002/admt.202000326.